

Supporting Information

Identification and characterizing the amyloid- β (42) oligomeric conformation and size targeting the receptor LirB2

Jinfei Mei, Wen Xu, Wenqi Gao, Chuanbo Wang, Yvning Guan Sajjad Ahmad and Hongqi Ai *

School of Chemistry and Chemical Engineering, University of Jinan, Jinan 250022, P.R. China

*To whom correspondence should be addressed, E-mail: chm_aihq@ujn.edu.cn

Contents

Model building and preparation	Pages S2-S3
Figures S1-S12	Pages S4-S18
Tables S1-S3	Pages S18-S19

Model building and preparation

The LDD receptor (PDB ID: 6BCS)¹, “U”-type (PDB ID: 2BEG)², “S”-type (PDB ID: 7Q4B/ 7Q4M) and “LS”-type³ (PDB ID: 5OQ V) Aβ42 fibril are from the RCSB database (<https://www.rcsb.org/>).

AβOs: These AβO were selected from different aggregation stages (The definition was based on the β-sheet content between Aβ42 peptide chains and the number of Aβ42 peptide chains): SP1: AβO species with ~10 % β-sheet content (~5 % intermolecular and ~5 % intramolecular β-sheet contents), including dimer (*D*), Trimer (*T*), Tetramer (*Te*), Pentamer (*P*), Hexamer (*H*) and Octamer (*O*) from our previous Aβ42 models⁴ to mimic various AβOs at the initial stage of aggregation. The tertiary structural features observed for these oligomers are supported by the study of Barz et al.⁵ SP2: secondary nucleated AβO species, with ~40 % intermolecular β-sheet content and consequently the relatively rigid peptide chains, including dimer (*D_T*), Trimer (*T_T*), Tetramer (*Te_T*) and Pentamer (*F_T*) of AβO in the secondary nucleated stage were built based on the models from AβO conformation reported in the literature^{6, 7}. SP3: initially nucleated AβO species, characterized in between the AβOs in the SP1 and SP2, in which four types of tetramers and pentamers with different intermolecular β-sheet contents were constructed, including 0 % intermolecular β-sheet and ca 33% total β-sheet contents (0 %, ~33 %), (~12 %, ~30.0 %), (~18 %, ~18 %), and (~25 %, ~25 %). The four kinds of tetramers and pentamers are abbreviated as Te-1/P-1, Te-2/P-2, Te-3/P-3 and Te-4/P-4 in Table S1. Moreover, these AβO species have two “toxicity turns” at residues “22-23” and “38-39”.

Aβ42 protofibrils/fibrils chains complement details: Chimera software was used to complement the defective “U”-type (PDB ID: 2BEG)² and “S”-type (PDB ID: 7Q4B/ 7Q4M)⁸ Aβ42 fibrils chain, and then performed the simulation annealing for the following model building, as did previously⁹. The initial structure of the Aβ42 fibrils of the completed peptide chain was first embedded in the cube box containing TIP3P water model with a margin of 10 Å, and then added sodium ions to keep it neutral. *SA details:* After energy minimization, a periodic algorithm is formulated for each

temperature group from the initial temperature (300 K) to the final temperature (500 K), and the algorithm is repeated throughout the simulation. The number of control temperature points was set to five, with annealing times of 0, 20, 60, 70 and 100 (ps) for each temperature and temperature values of 300 K, 500 K, 500 K, 300 K and 300 K, respectively. After 100 such annealing cycles (10 ns), the “U”-type and “S”-type A β 42 protofibrils with flexible and relaxed ends were obtained.

Protein-Protein Docking Use the “Cluspro 2.0” website,¹⁰ which employed “Fast Fourier Transform” to sample billions of conformations of the receptor and ligand through rigid docking, and ultimately obtained 1000 lowest energy complex structures. The 1000 complex structures were then further analyzed via the root mean square deviation (RMSD) to obtain the 30 most representative complex models. Finally, we used the “Energy Minimization Scoring” module to select three ideal complex structures (Figs.S1-1, S2, S3). In addition, in order to verify Cluspro results, we also used “HDOCK”¹¹ server for protein-protein docking, and the results are shown in the Fig.S1-2. The results of “HDOCK” showed that the I region of LDD receptor was also a suitable binding site for low-MW A β O, and the II/III region was more suitable for the high-MW A β O.

MM/PBSA script specific parameter Frames (0.1 ns for one sample), time scale (last 10 ns), solvation models (continuum model). We utilized an enhanced script for calculating the binding energy, sourced from https://jerkwin.github.io/2021/03/16/gmx_mmpbsa_script_updates - shielding effect and the entropy contribution/. The script considers not only the ionic strength but also incorporates the Debye characteristic length to calculate ΔE_{cou} , resulting in an exponential decay of the electrostatic interaction.¹²⁻¹⁴

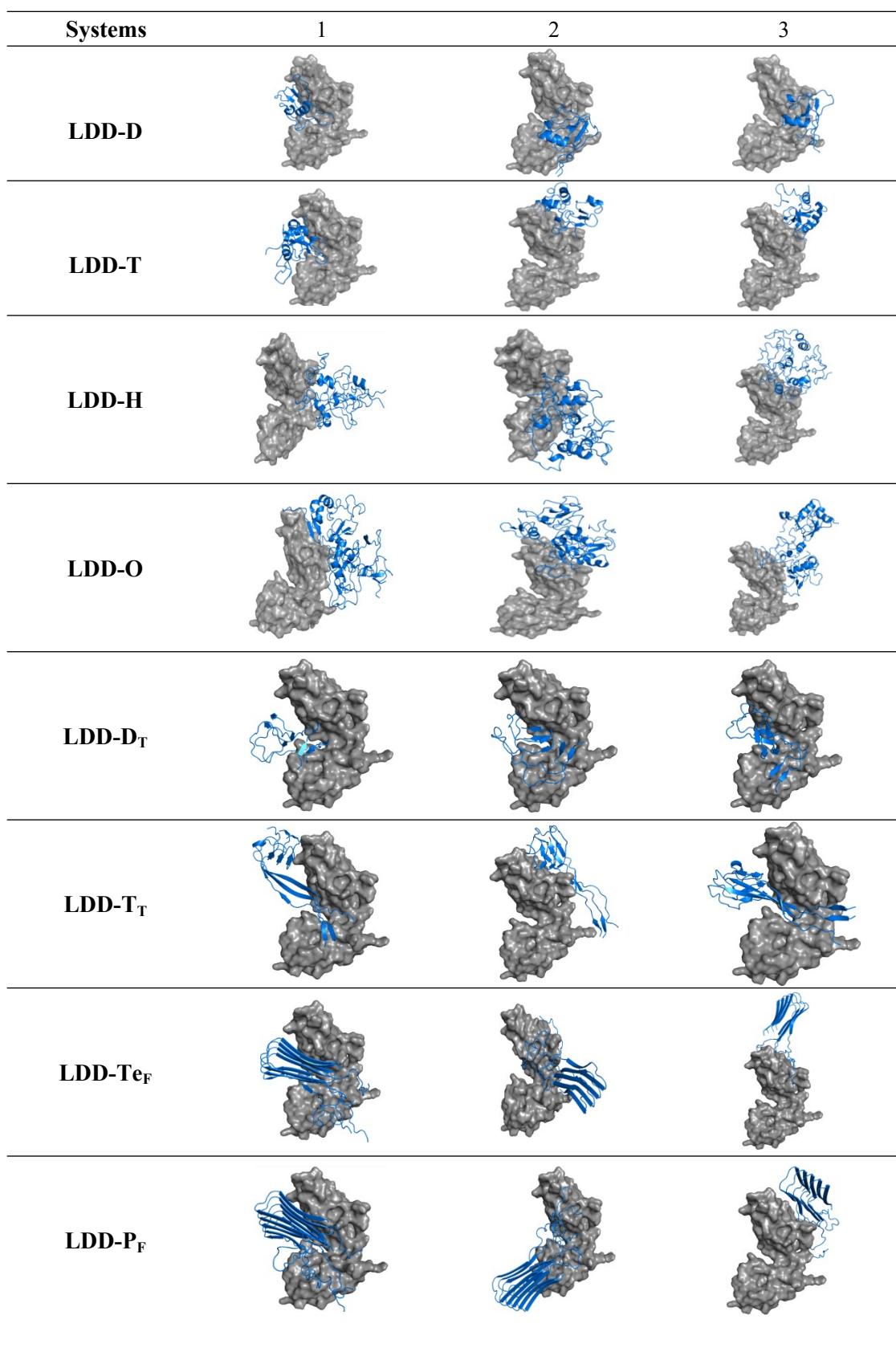
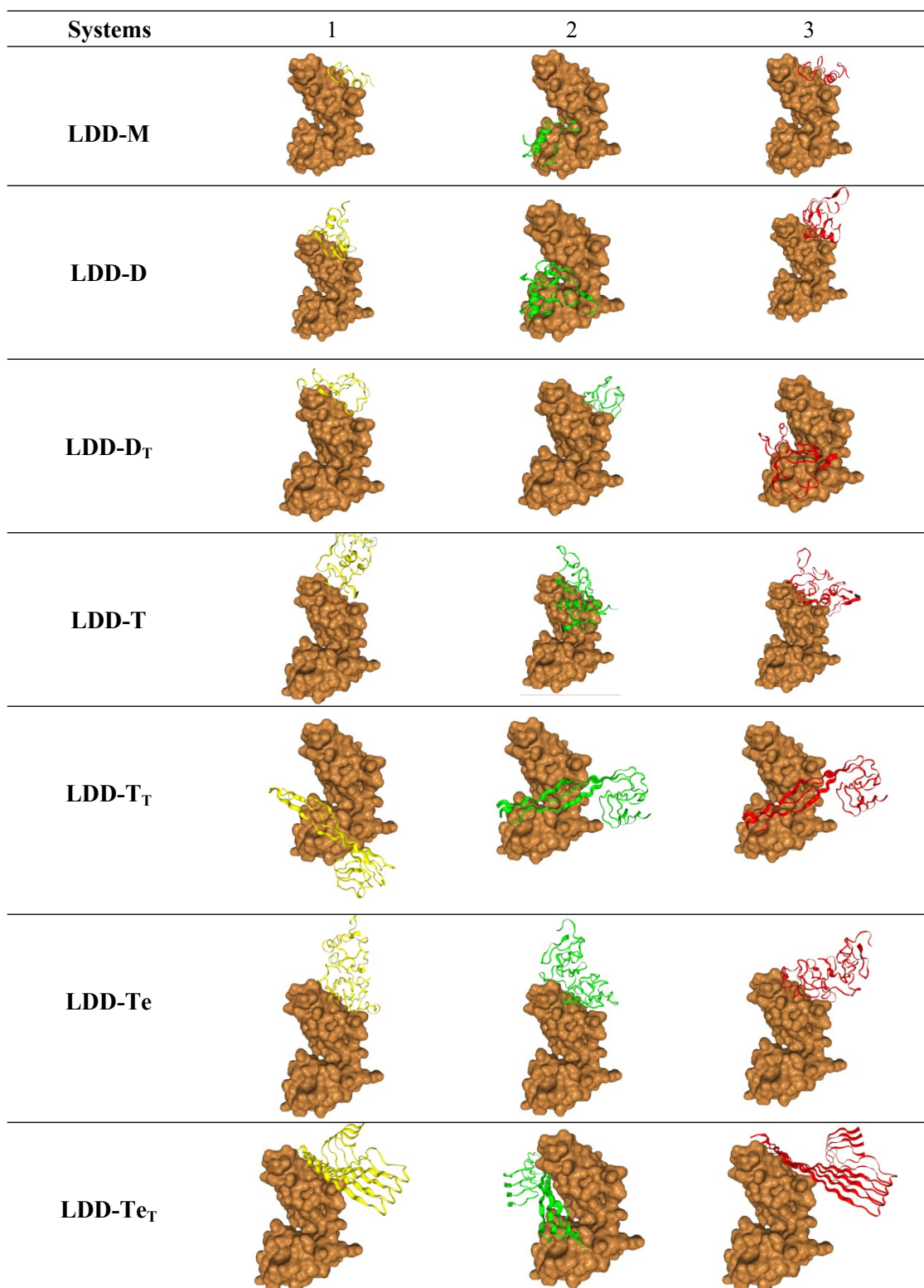


Fig. S1-1 The initial top3 models for each A β O(1-40) -LDD interaction ranked by "ClusPro" website.



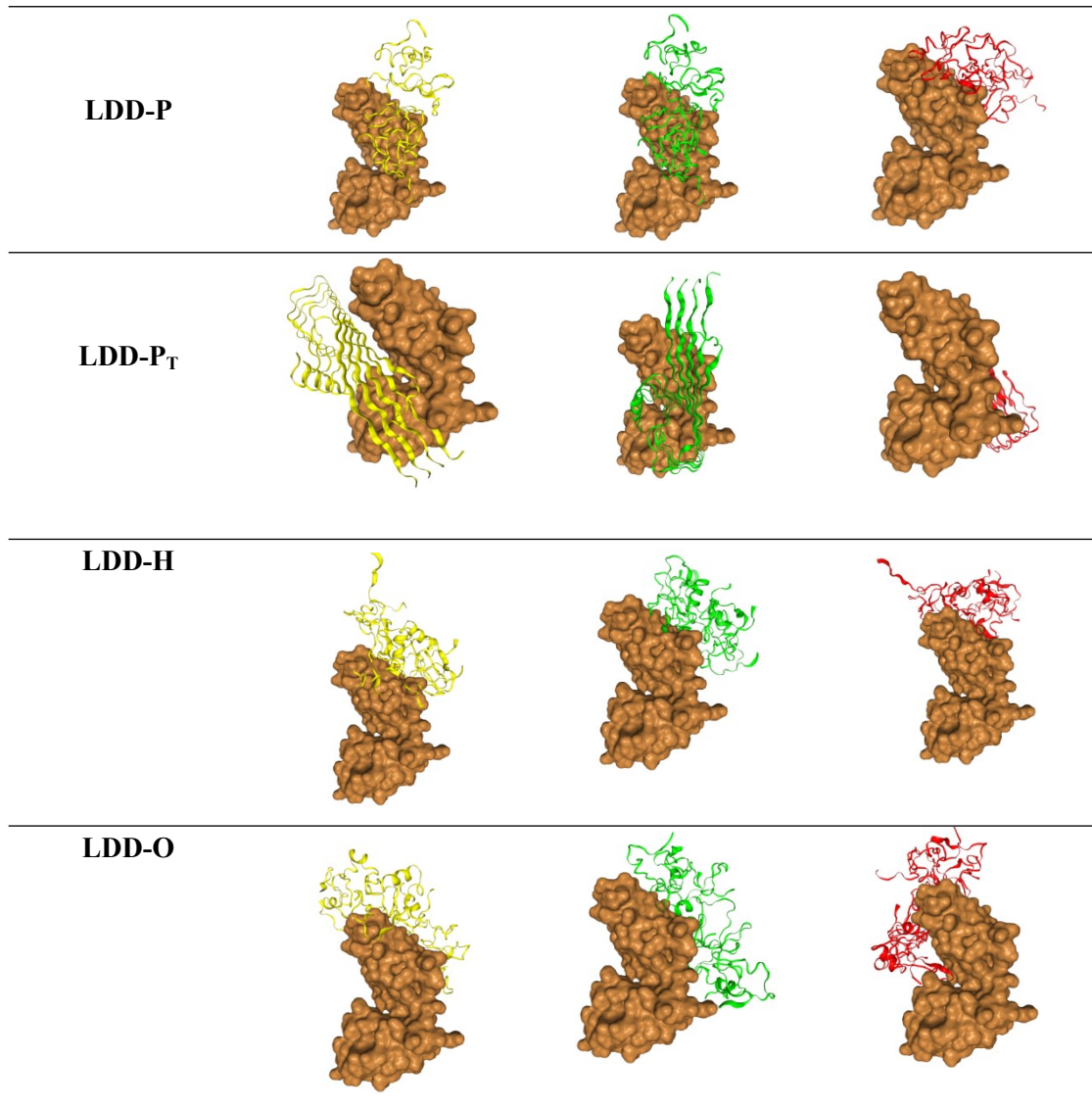
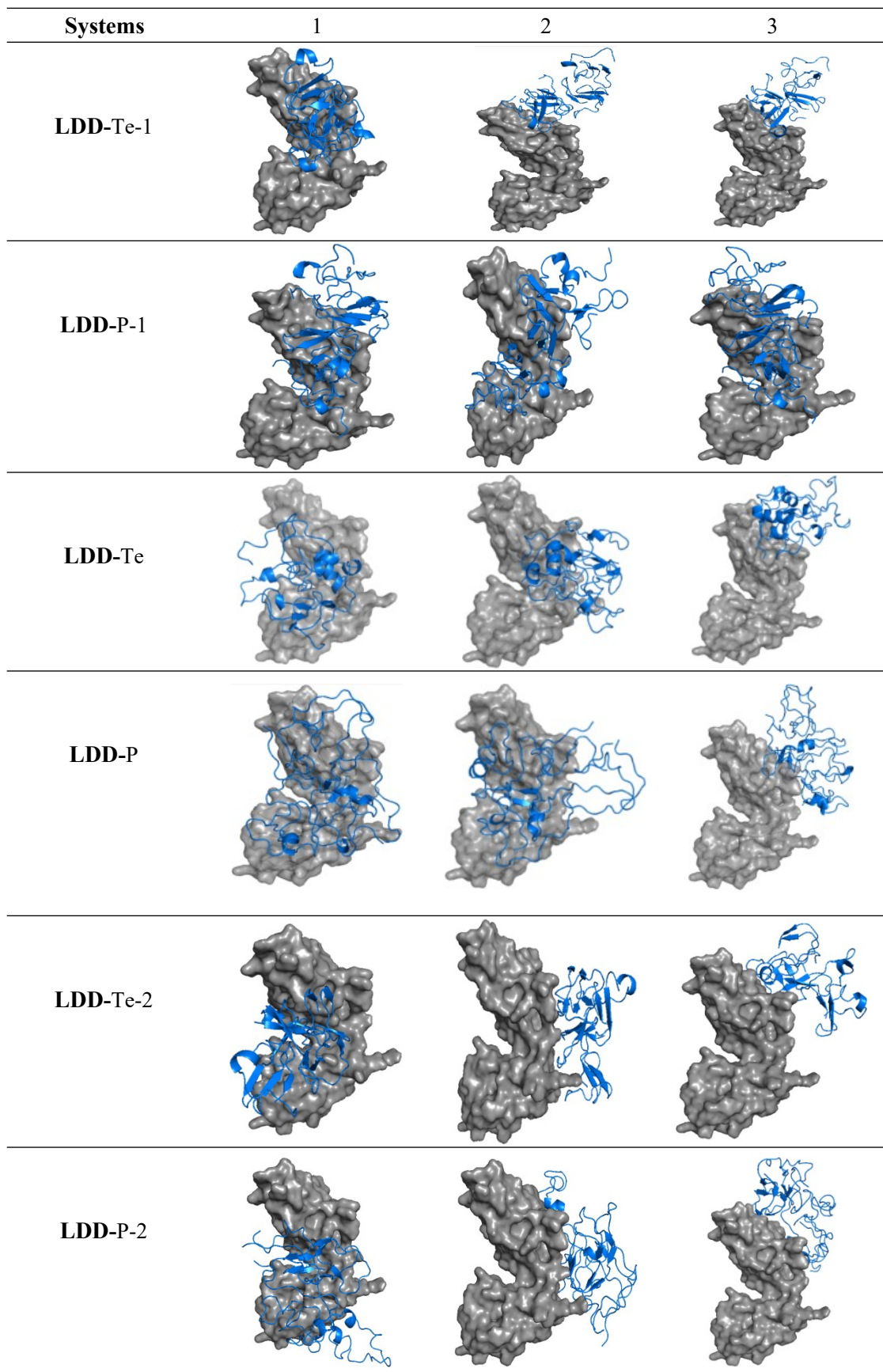


Fig. S1-2 The initial top3 models for each A β O-LDD interaction ranked by “HDOCK” website.



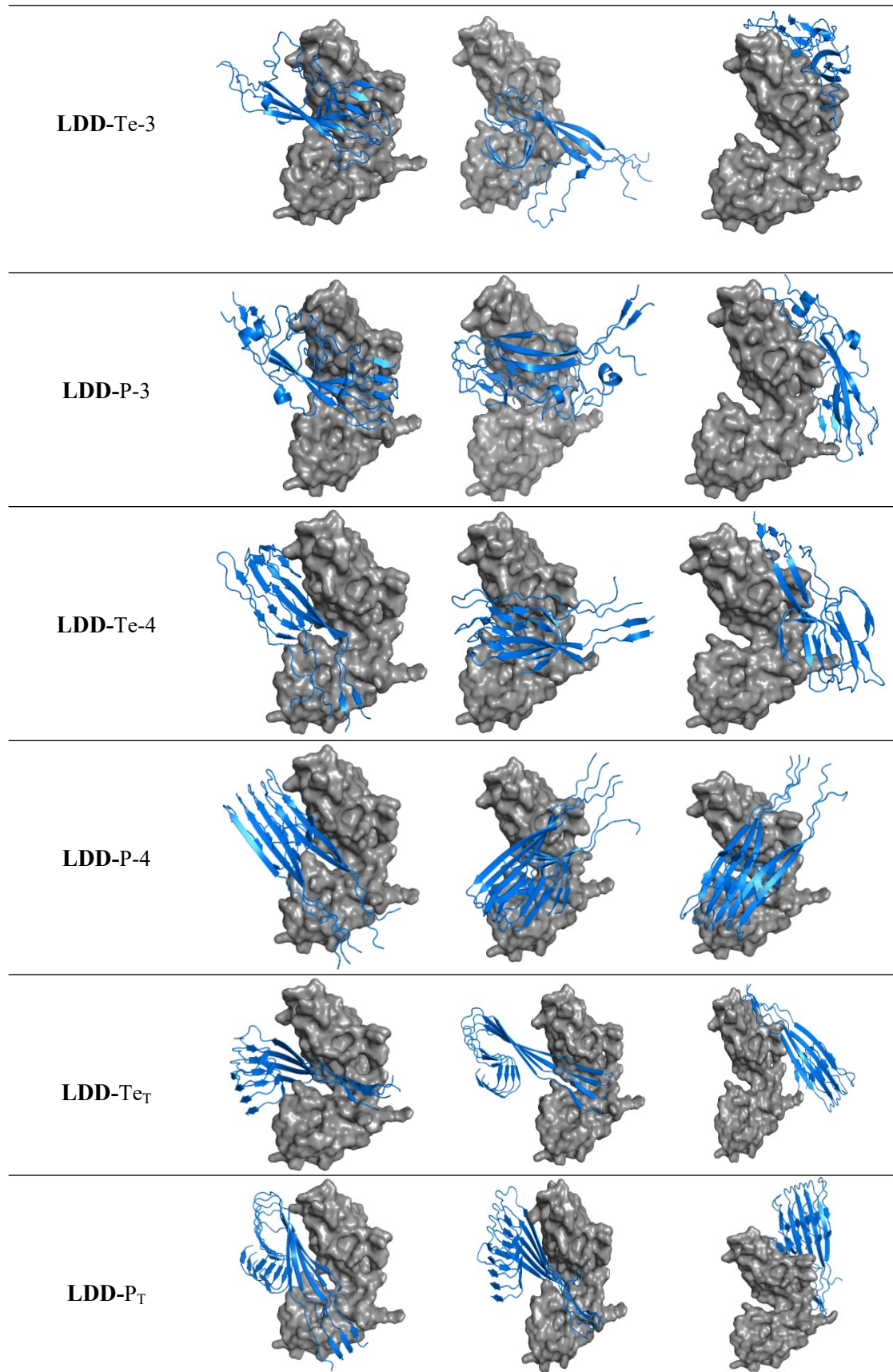
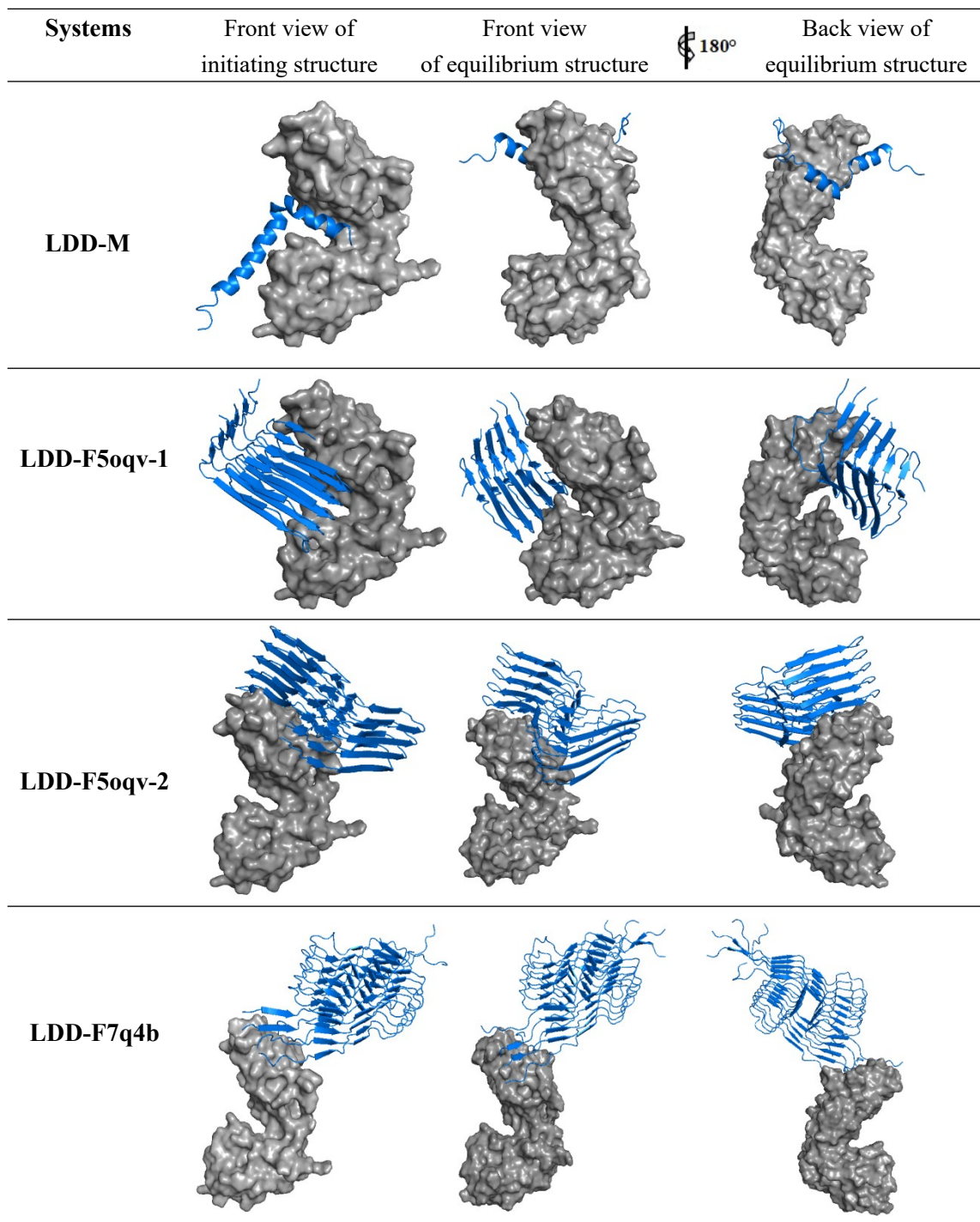
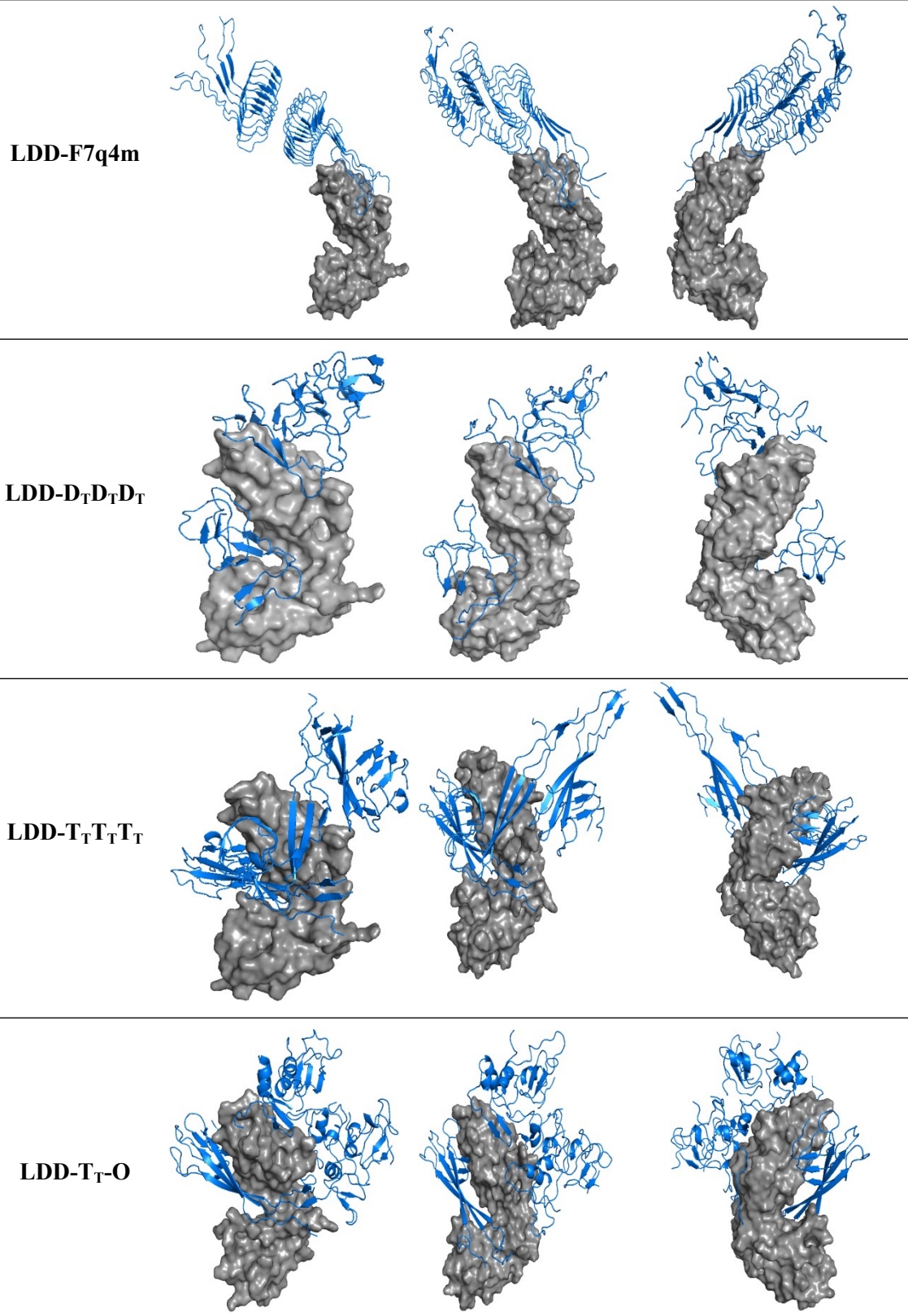


Fig. S2 The initial top3 models for each model of tetramer (Te)/pentamer (P) (SP1, SP2, SP3) bound LDD receptor, ranked by “ClusPro” website.





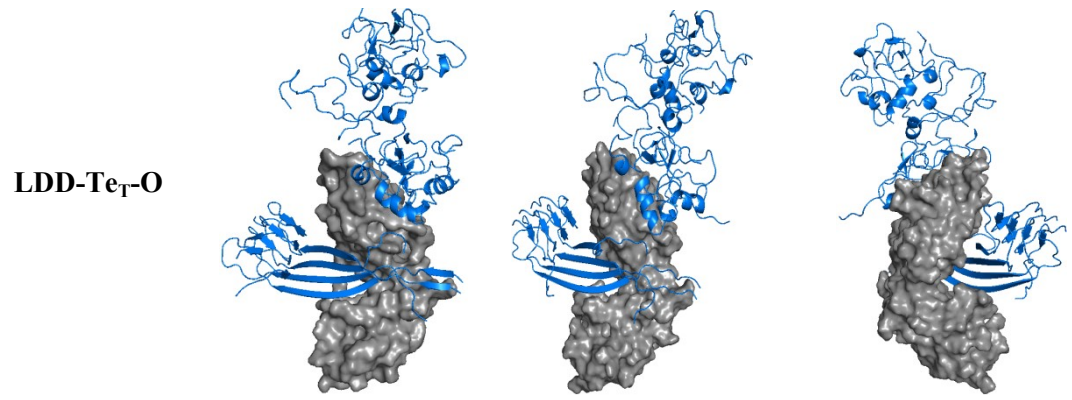
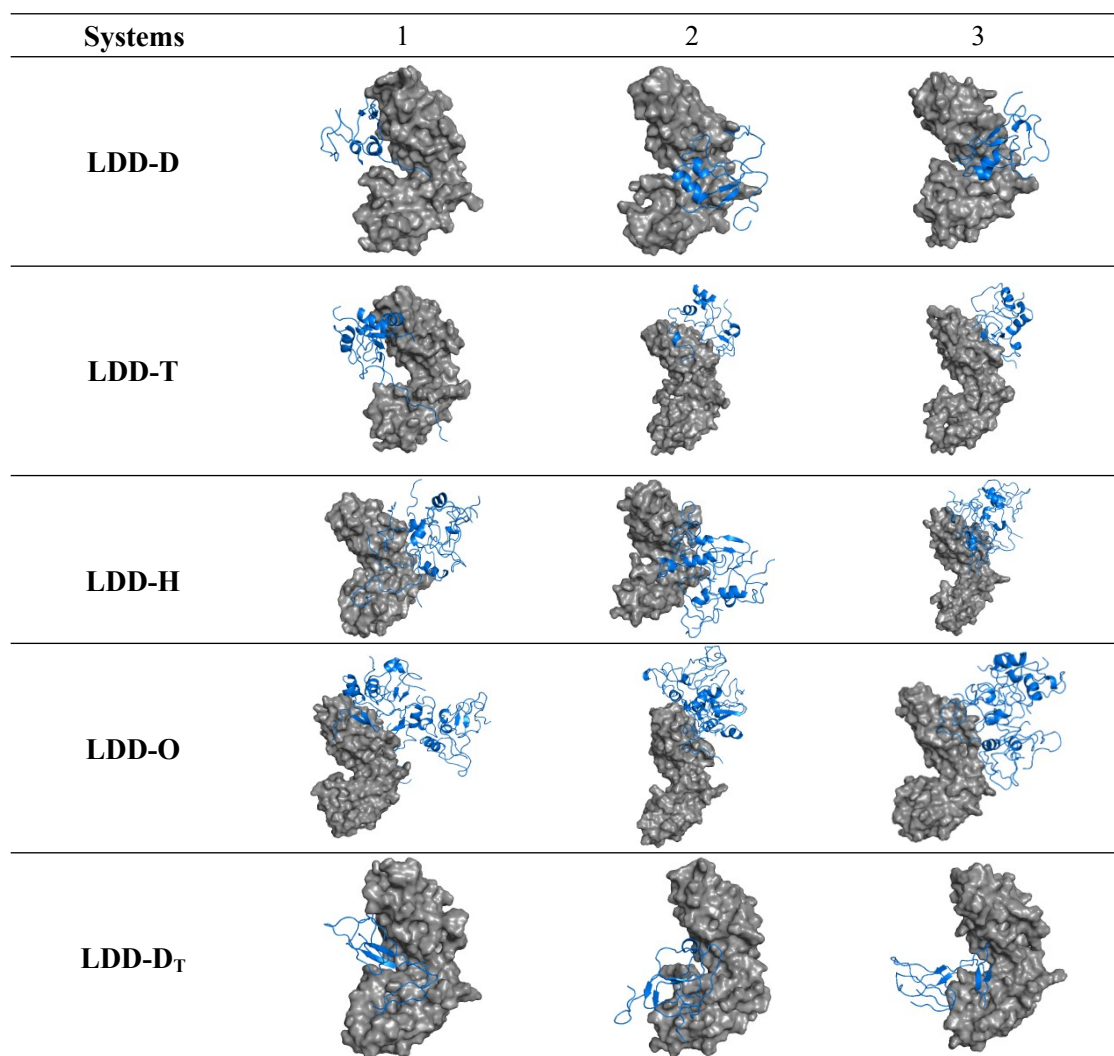


Fig. S3 Conformations of LDD-A β O (SP1, SP2, SP4) complexes at initial (2nd column) and equilibrium (3rd-4th columns) states.



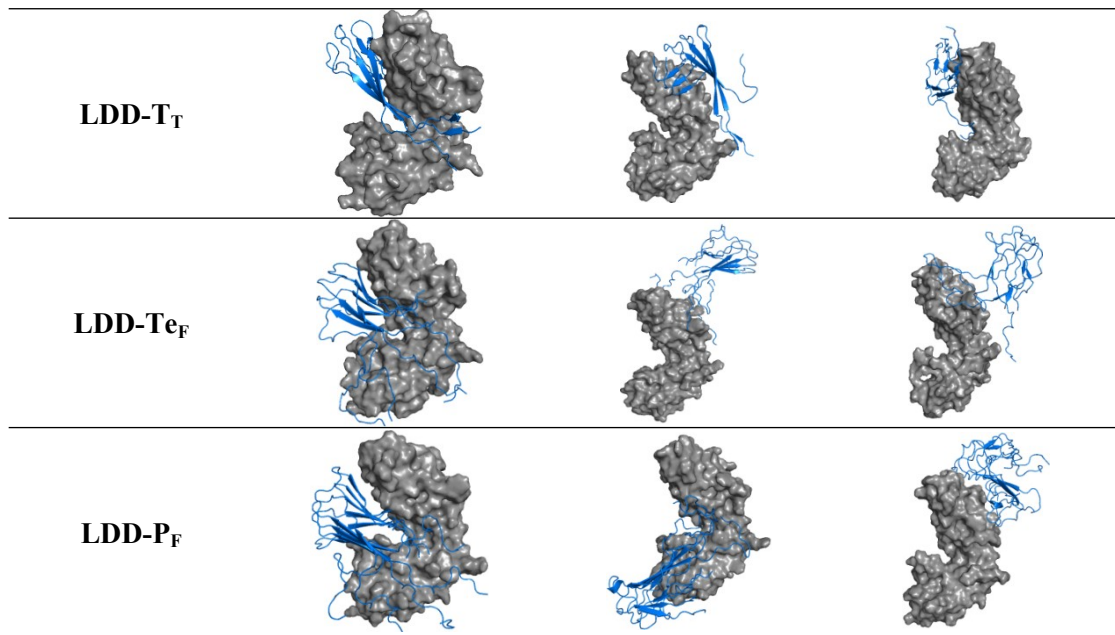
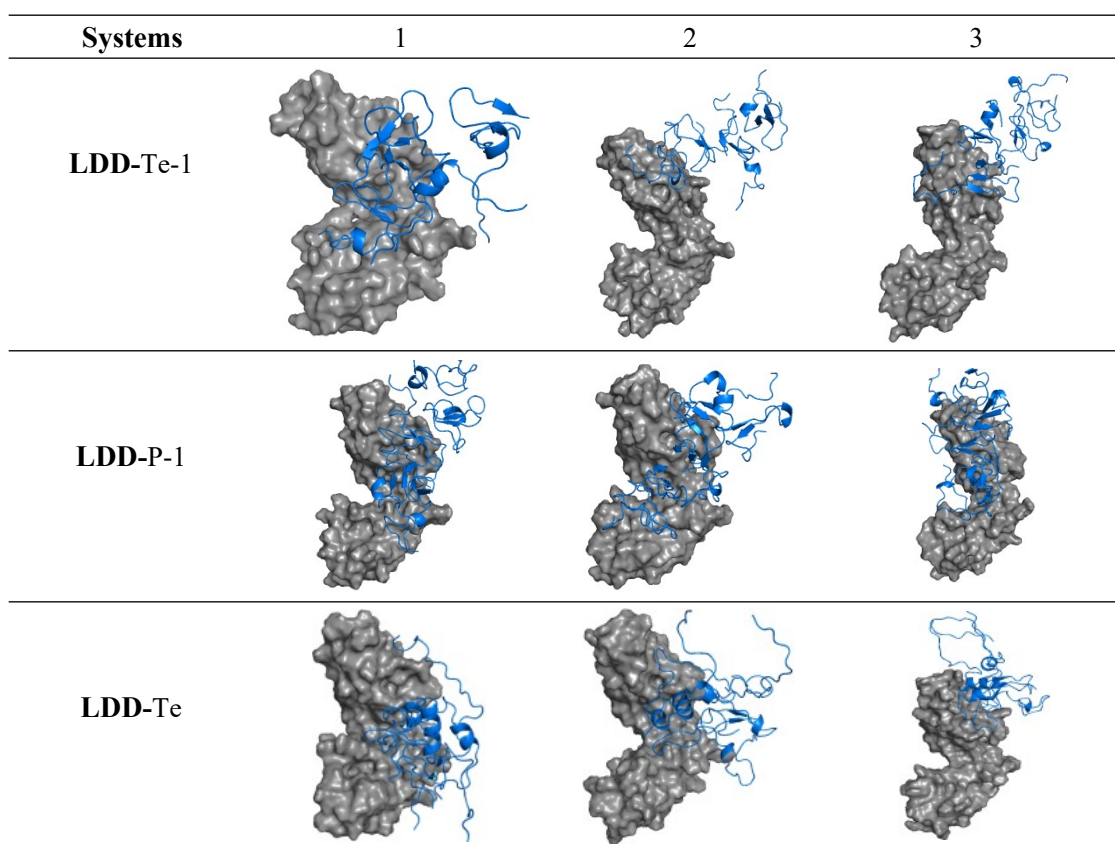
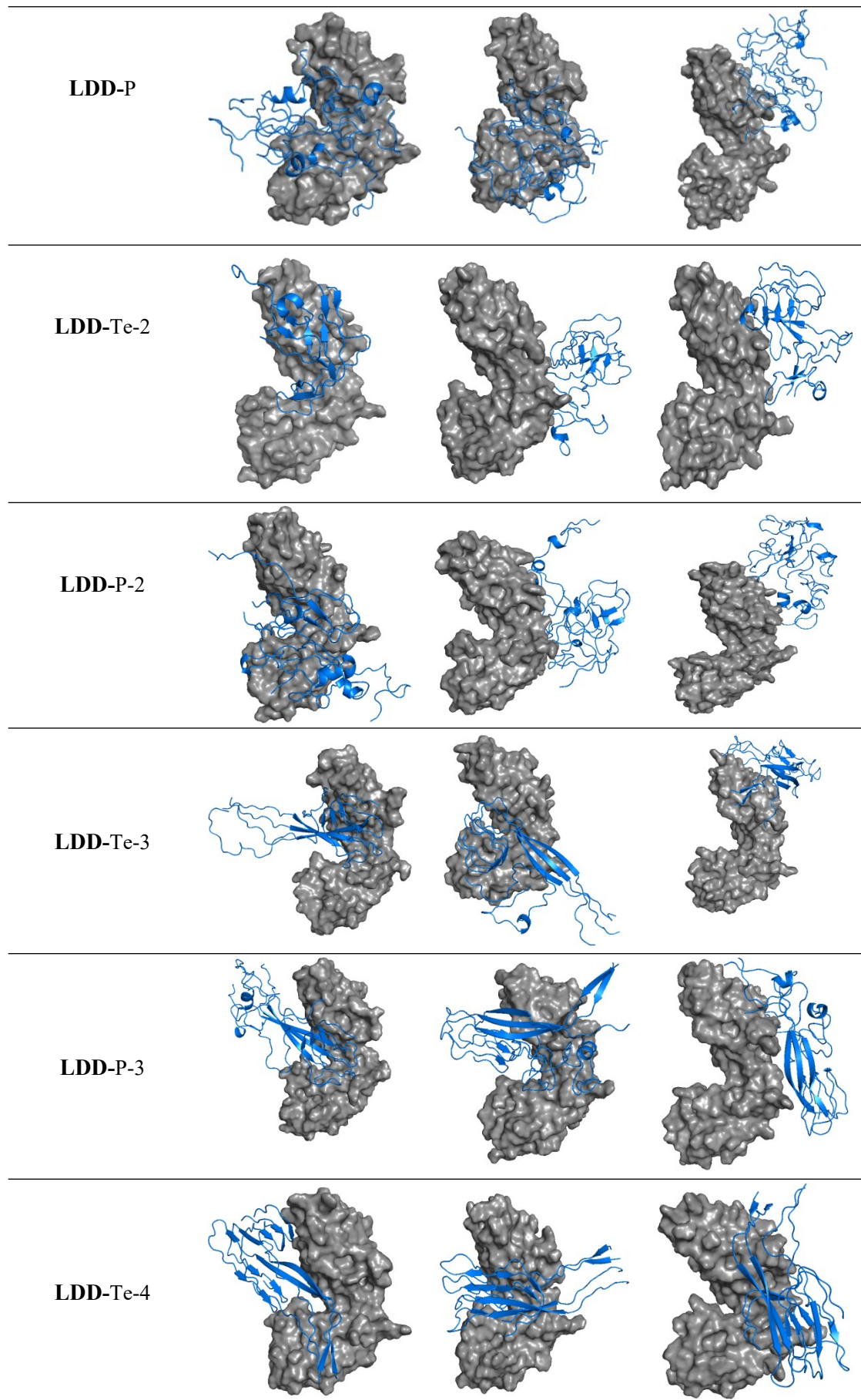


Fig. S4 Top 3 conformations of each LDD-A β O complexes (SP1, SP2, SP4) at equilibrium states.





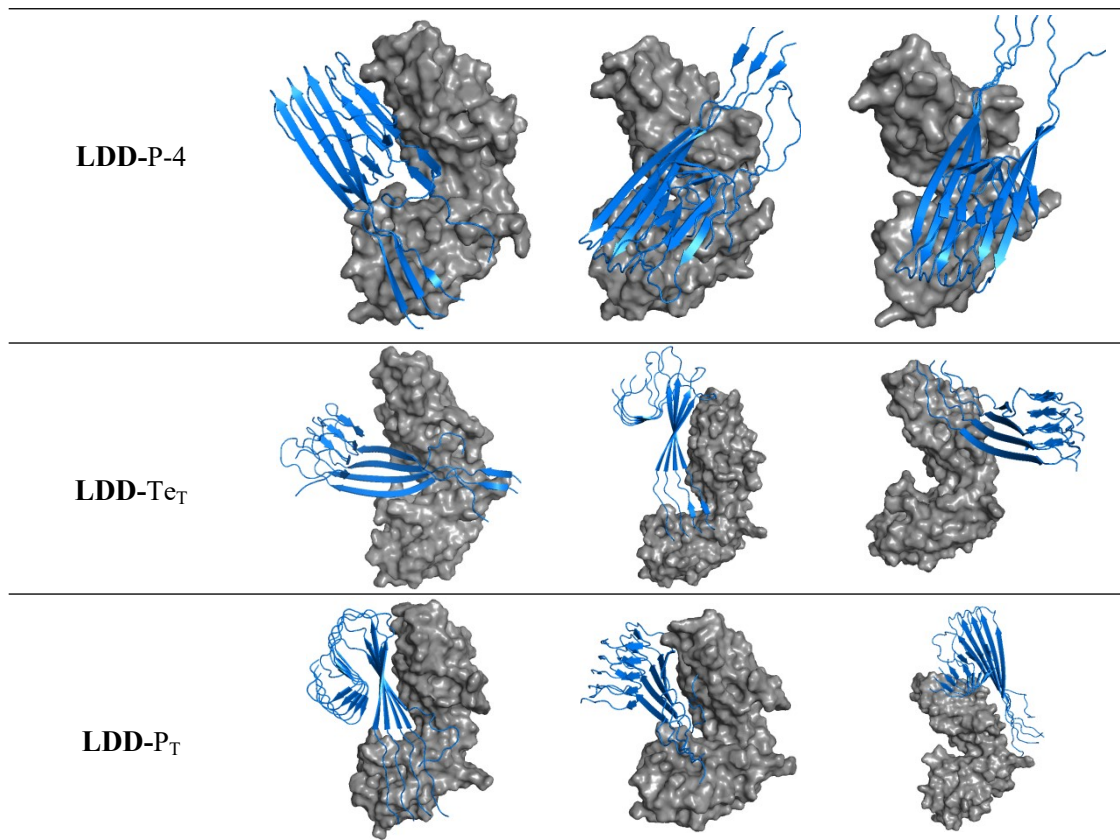


Fig. S5 Top 3 conformations for each model of tetramer (Te)/pentamer (P) (SP1, SP2, SP3) bound LDD receptor complexes at equilibrium states.

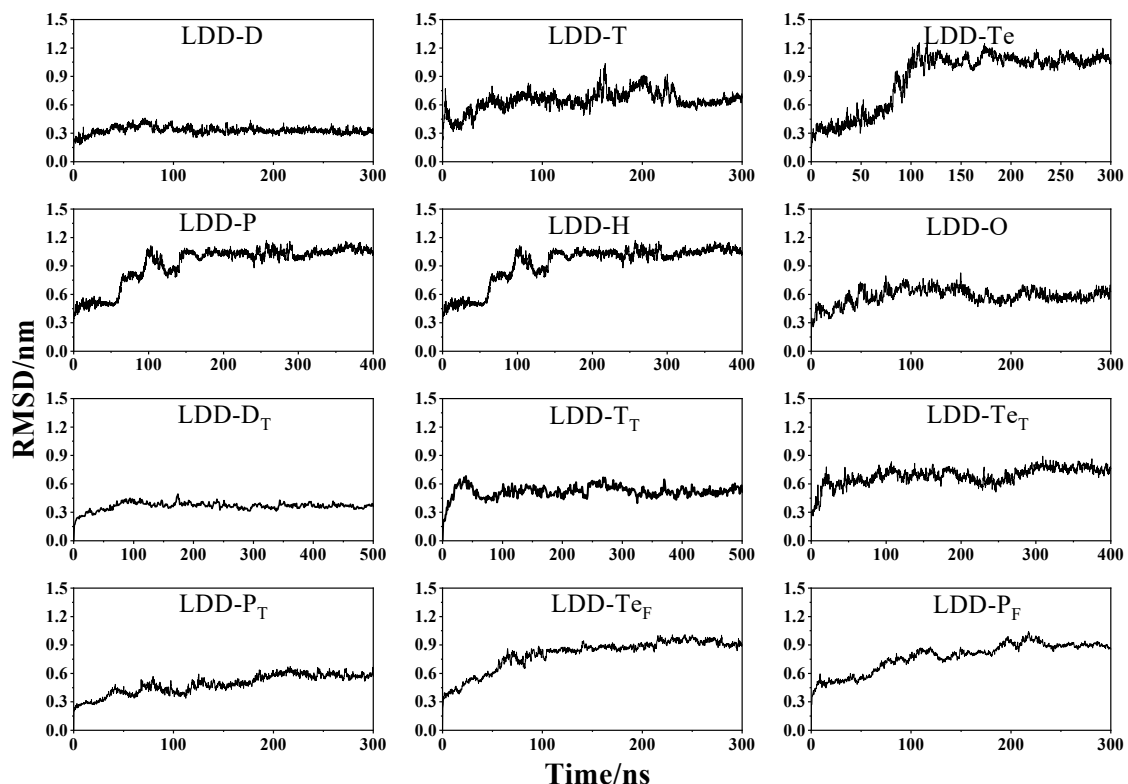


Fig. S6 The RMSD of the complex formed by A β O and LDD.

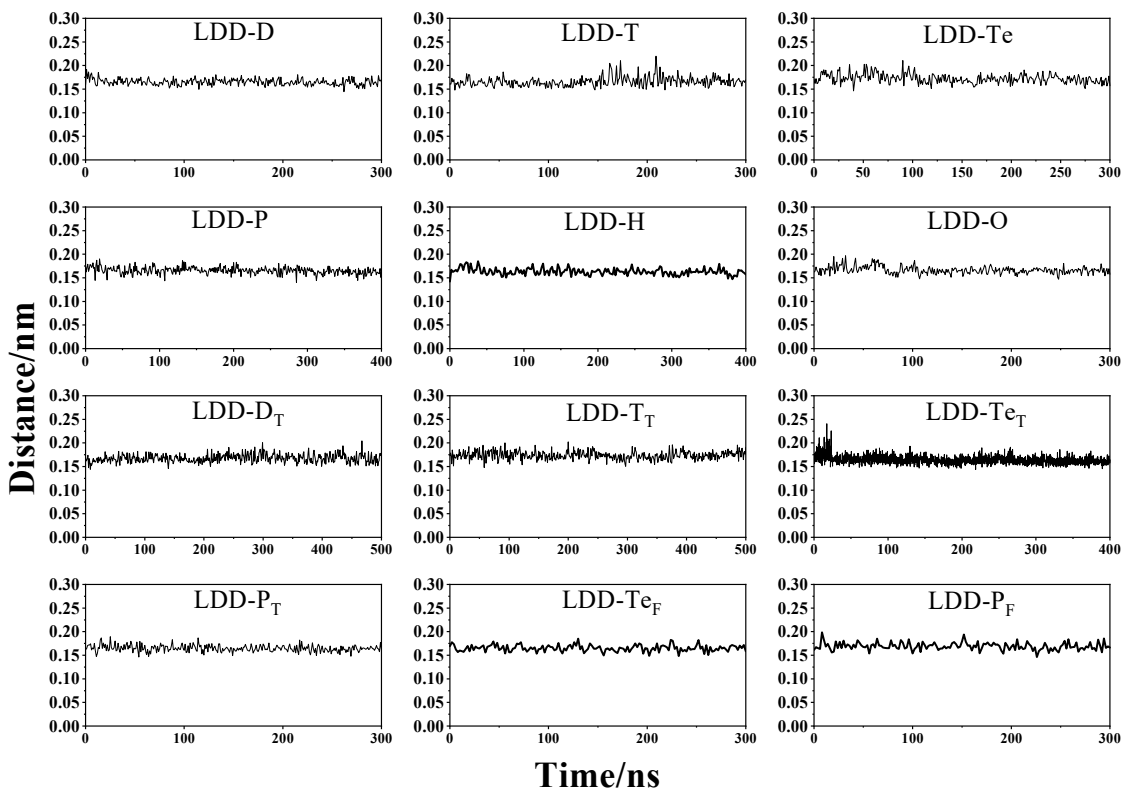


Fig. S7 Microprocesses of minimum distance between A β O and the LDD "initial Docking site" during the equilibrium simulation.

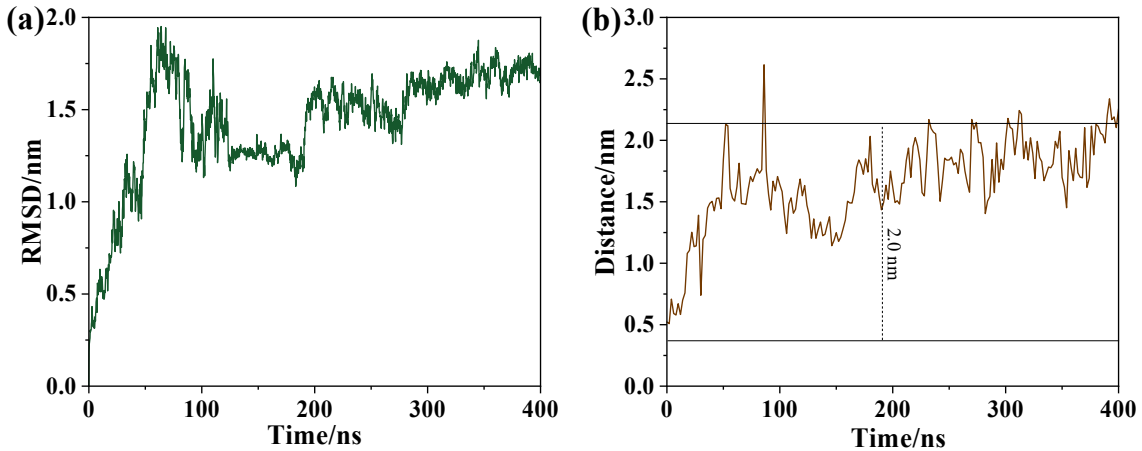


Fig. S8 The RMSD of the complex formed by A β 42 monomer and LDD(a), and microprocesses of minimum distance between A β 42 monomer and the LDD "initial Docking site" during the equilibrium simulation(b).

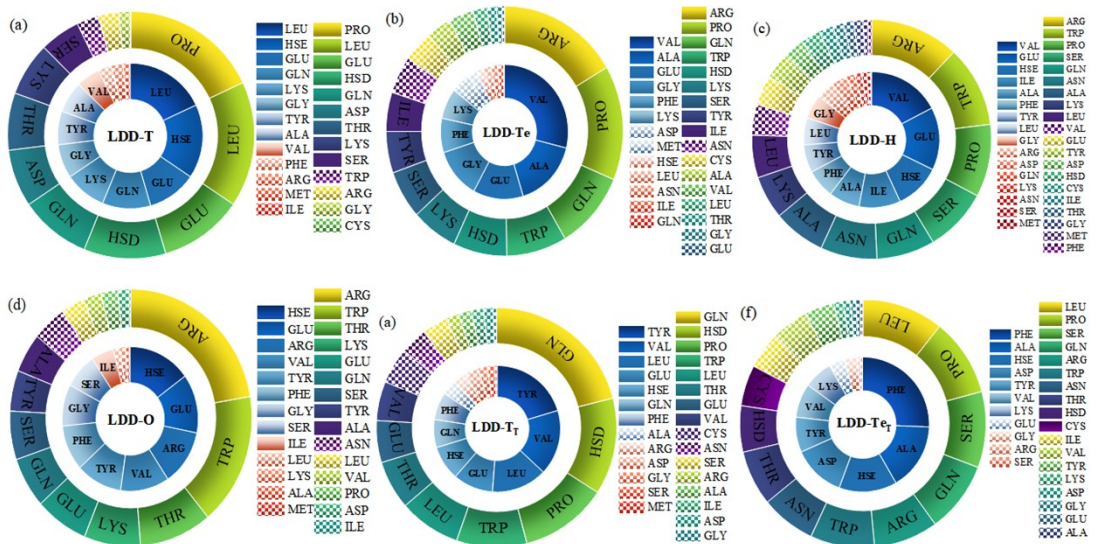


Fig. S9 The probability of residues contributing to the contact interface of A β O (inner torus)-LDD (outer torus) complexes. The residues with less (<~5 %) contact contributions are represented by mosaic. The residues on the contact interface are highlighted in light color, embedding in the deep-blue surface. A β O species involved in complexes (a-f) are T, Te, H, O, T_t and Te_t, respectively.

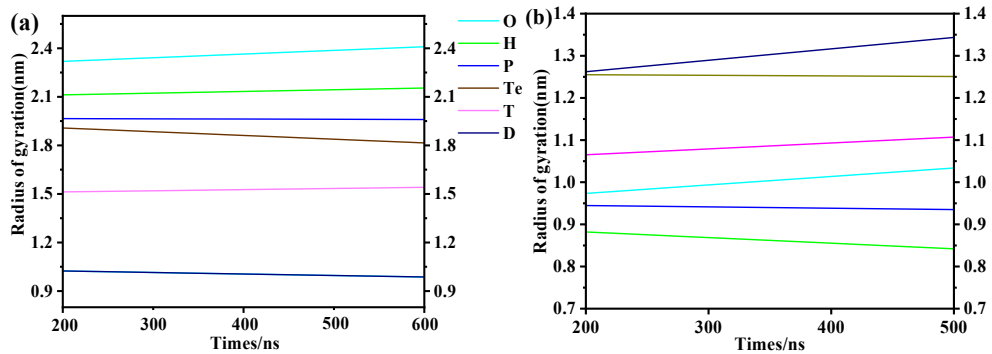


Fig. S10-1 The variation of the gyration radius of A β 42 oligomers in the A β O-LDD complex with time after linear fitting.

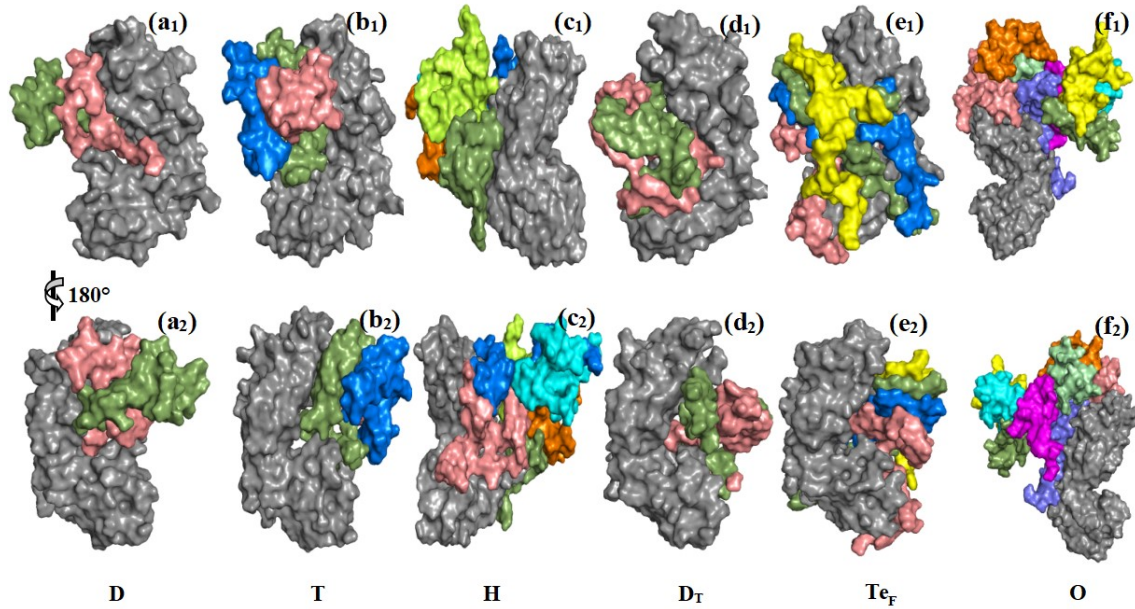


Fig. S10-2 3D contact map of LDD and A β 42 oligomers. Gray is LDD, green, yellow and blue are A β 42 oligomers/fibril peptide chain; (a₁₋₂), (d₁₋₂) and (e₁₋₂) represent LDD-D, T, D_T and T_f bound to LDD I binding region, respectively; (b₁₋₂) represents LDD-H bound to LDD II binding region; (c₁₋₂) represents LDD-O bound in the LDD III binding region.

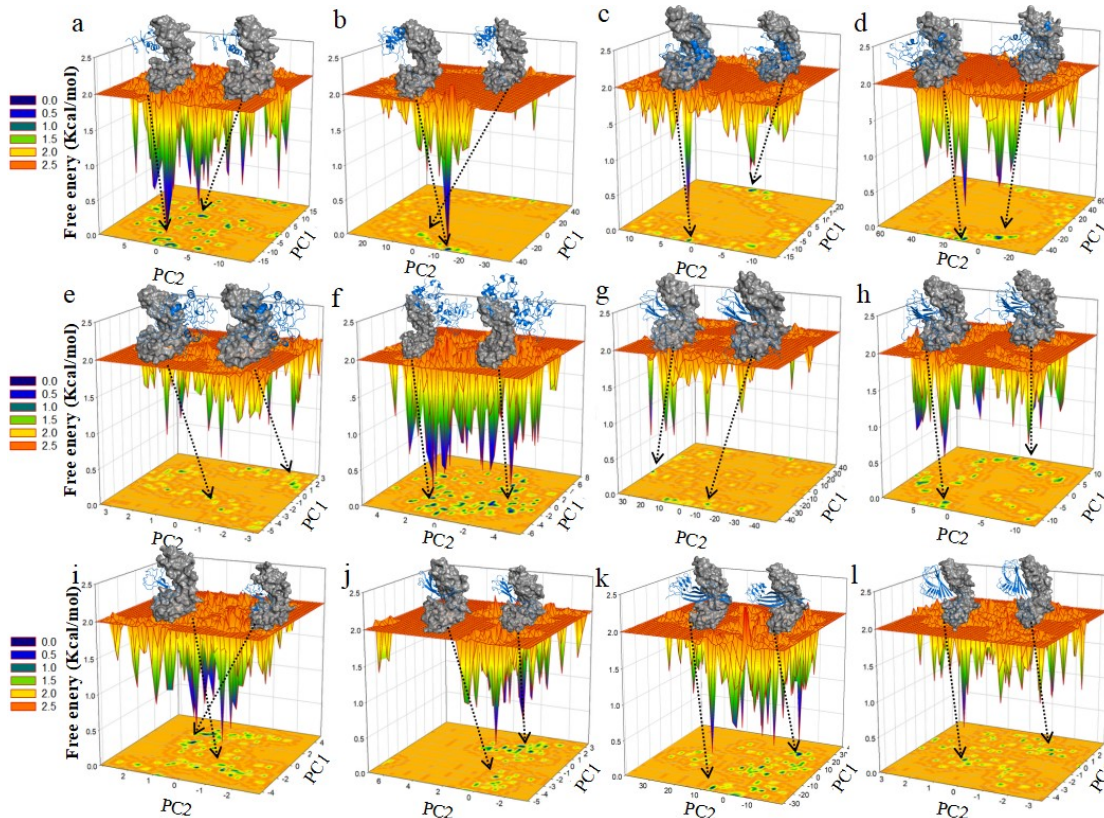


Fig. S11 3D/2D free energy landscapes of the LDD – A β O complexes, the PC1 and PC2 are the

two largest eigenvectors. a-f represents LDD - A β 42 D/T/Te/P/H/O respectively, g-h represents LDD - A β 42 Te_F/P_F respectively, and i-l represents D_T/T_T/Te_T/P_T respectively. On each figure, the model with the lowest energy is depicted on the left, while the model with the next lowest energy is shown on the right.

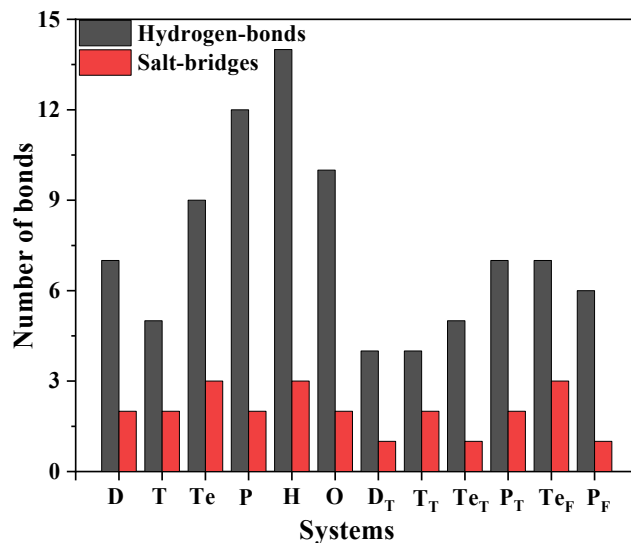


Fig. S12 Number of hydrogen-bond and salt-bridge in total A β O-LDD.

Table S1-1. The β -sheet content (%) of A β O at four characteristic subphases.

Systems	SPs	Intramolecular β -sheet (%)	Intermolecular β -sheet (%)	Total β -sheet (%)	Regions of A β O binding
LDD-D	SP(1)	10.3	6.4	16.7	Region I
LDD-T	SP(1)	8.1	8.6	16.7	Region I
LDD-H	SP(1)	7.0	6.1	13.1	Region II
LDD-O	SP(1)	0.4	7.6	8.0	Region III
LDD-D _T	SP(2)	4.0	36.2	40.2	Region I
LDD-T _T	SP(2)	0	42.3	42.3	Region I
LDD-Te _F	SP(4)	0	45.8	45.8	Region I
LDD-P _F	SP(4)	0	46.2	46.2	Region I
LDD-F5oqv1	SP(4)	0	83.3	83.3	Region I
LDD-F5oqv-2	SP(4)	0	88.6	88.6	Region III
LDD-F7q4b	SP(4)	0	74.7	74.7	Region III
LDD-F7q4m	SP(4)	0	75.8	75.8	Region III

Table S1-2. The β -sheet content (%) of all the constructed tetramers (Te) and pentamers (P) at the SP3.

Systems	Intramolecular β -sheet (%)	Intermolecular β -sheet (%)	Total β -sheet (%)	Regions of A β O binding
LDD-Te-1	33.3	0	33.3	Region II
LDD-P-1	32.1	0	32.1	Region II
LDD-Te	6.0	5.8	11.4	Region II
LDD-P	5.4	6.0	13.3	Region II
LDD-Te-2	17.8	11.9	29.7	Region II
LDD-P-2	17.1	11.4	28.5	Region II
LDD-Te-3	0	18.5	18.5	Region I
LDD-P-3	0	18.0	18.0	Region I
LDD-Te-4	0	24.4	24.4	Region I
LDD-P-4	0	27.6	27.6	Region I
LDD-Te _T	0	38.1	38.1	Region I
LDD-P _T	0	36.2	36.2	Region I

Table S2. The binding energy (kcal/mol) / dissociation constant(mol/L) between the LDD receptor and A β fibril.

Systems	ΔG_{PB}	ΔG_{SA}	ΔE_{COU}	ΔE_{VDW}	$-T\Delta S$	ΔG_{bind}	$\Delta G_{bindfit}$	K_d	Regions
LDD-F5oqv-1	221.9	-12.9	-167.2	-81.9	15.8	-24.3	-12.9	3.4×10^{-10}	I
LDD-F5oqv-2	170.3	-8.7	-184.9	-42.3	36.7	-28.9	-8.2	9.6×10^{-7}	III
LDD-F7q4b	269.3	-11.8	-212.2	-74.6	26.6	-2.7	-10.4	2.3×10^{-8}	III
LDD-F7q4m	202.1	-13.8	-148.4	-78.2	33.9	-4.4	-10.4	2.3×10^{-8}	III

Table S3. Relative difference between the first and second lowest free energies (kcal·mol⁻¹) of the LDD-A β O complexes.

Complexes	LDD-D	LDD-T	LDD-Te	LDD-P	LDD-H	LDD-O	LDD-Te _F	LDD-P _F	LDD-D _T	LDD-T _T	LDD-Te _T	LDD-P _T
Relative difference	0.50	0.95	0.74	0.25	0.40	0.09	0.02	0.13	0.29	0.46	0.30	0.45

References:

1. Q. Cao, W. S. Shin, H. Chan, C. K. Vuong, B. Dubois, B. Li, K. A. Murray, M. R. Sawaya, J. Feigon, D. L. Black, D. S. Eisenberg and L. Jiang, *Nat. Chem.*, 2018, **10**, 1213-1221.
2. T. Lührs, C. Ritter, M. Adrian, D. Riek-Lohr, B. Bohrmann, H. Döbeli, D. Schubert and R. Riek, *Proc. Natl. Acad. Sci. U S A*, 2005, **102**, 17342-17347.
3. L. Gremer, D. Schölzel, C. Schenk, E. Reinartz, J. Labahn, R. B. G. Ravelli, M. Tusche, C. Lopez-Iglesias, W. Hoyer, H. Heise, D. Willbold and G. F. Schröder, *Science*, 2017, **358**, 116-119.
4. J. Mei, H. Yang, S. Ahmad, X. Ma, W. Xu, W. Gao, Y. Li, C. Wang and H. Ai, *ACS Chem. Neurosci.*, 2022, **13**, 2048-2059.
5. B. Barz, Q. Liao and B. Strodel, *J. Am. Chem. Soc.*, 2018, **140**, 319-327.
6. Y. Irie, K. Murakami, M. Hanaki, Y. Hanaki, T. Suzuki, Y. Monobe, T. Takai, K.-i. Akagi, T. Kawase, K. Hirose and K. Irie, *ACS Chem. Neurosci.*, 2017, **8**, 807-816.
7. K. Murakami, K. Irie, H. Ohigashi, H. Hara, M. Nagao, T. Shimizu and T. Shirasawa, *J. Am. Chem. Soc.*, 2005, **127**, 15168-15174.
8. Y. Yang, D. Arseni, W. Zhang, M. Huang, S. Lövestam, M. Schweighauser, A. Kotecha, A. G. Murzin, S. Y. Peak-Chew, J. Macdonald, I. Lavenir, H. J. Garringer, E. Gelpi, K. L. Newell, G. G. Kovacs, R. Vidal, B. Ghetti, B. Ryskeldi-Falcon, S. H. W. Scheres and M. Goedert, *Science*, 2022, **375**, 167-172.
9. H. Yang, J. Mei, W. Xu, X. Ma, B. Sun and H. Ai, *Phys. Chem. Chem. Phys.*, 2022, DOI: 10.1039/D2CP00569G.
10. I. T. Desta, K. A. Porter, B. Xia, D. Kozakov and S. Vajda, *Structure*, 2020, **28**, 1071-1081.e1073.
11. H. Li, E. Huang, Y. Zhang, S.-Y. Huang and Y. Xiao, *Protein Science*, 2022, **31**, e4441.
12. S. Genheden and U. Ryde, *Expert Opin Drug Discov*, 2015, **10**, 449-461.
13. K. Colwill, Y. Galipeau, M. Stuible, C. Gervais, C. Arnold, B. Rathod, K. T. Abe, J. H. Wang, A. Pasculescu, M. Maltseva, L. Rocheleau, M. Pelchat, M. Fazel-Zarandi, M. Iskilova, M. Barrios-Rodiles, L. Bennett, K. Yau, F. Cholette, C. Mesa, A. X. Li, A. Paterson, M. A. Hladunewich, P. J. Goodwin, J. L. Wrana, S. J. Drews, S. Mubareka, A. J. McGeer, J. Kim, M. A. Langlois, A. C. Gingras and Y. Durocher, *Clin Transl Immunology*, 2022, **11**, e1380.
14. H. Sun, Y. Li, S. Tian, L. Xu and T. Hou, *Phys. Chem. Chem. Phys.*, 2014, **16**, 16719-16729.